ACS APPLIED MATERIALS & INTERFACES

LETTER

www.acsami.org

Reversible Tuning of Plasmon Coupling in Gold Nanoparticle Chains Using Ultrathin Responsive Polymer Film

Saide Z. Nergiz and Srikanth Singamaneni*

Department of Mechanical Engineering and Materials Science, Washington University, St. Louis, Missouri 63130, United States

Supporting Information

ABSTRACT: We demonstrate large and reversible tuning of plasmonic properties of gold nanoparticles mediated by the reversible breaking and making of linear and branched chains of gold nanoparticles adsorbed on an ultrathin (1 nm) responsive polymer film. Atomic force microscopy revealed that at pH below the isoelectric point of the polybase (extended state of the polymer chains), gold nanoparticles adsorbed on the polymer layer existed primarily as individual nanoparticles. On the other hand, at higher pH, the polymer chains transition from coil to globule (collapsed) state, resulting in the formation of linear and branched chains with strong interparticle plasmon coupling. Reversible aggregation of the nanoparticles resulted in large and reversible change in the optical properties of the metal nanostructure assemblies. In particular, we observed a large redistribution of the intensity between the individual and coupled plasmon bands and a large shift (nearly 95 nm) in the coupled plasmon band with change in pH. Large tunability of plasmonic properties of the metal nanostructure chains reported here is believed to be caused by the chain aggregates of nanoparticles and un-cross-linked state of the adsorbed polymer enabling large changes in polymer chain conformation.

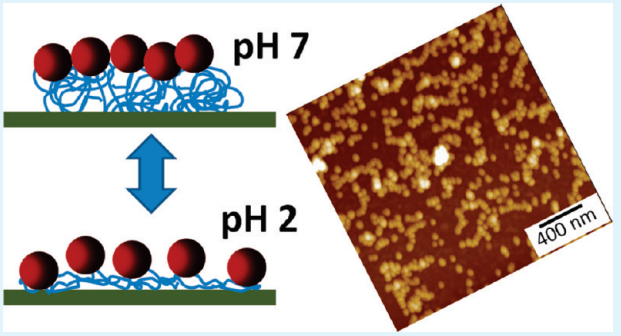

KEYWORDS: responsive plasmonics, gold nanoparticles, localized surface plasmon resonance, responsive polymer, nanoparticle chains

Surface plasmon involves the collective coherent oscillation of the conductive electrons at the interface of a metal and dielectric. A broad term, plasmonics involves the control of light at the nanoscale using surface plasmons,[1,2] which encompasses such unique optical phenomena as highly localized enhancement of electromagnetic (EM) field at nanostructured metal surface,[3,4] high sensitivity of the surface plasmon resonance to external medium,[5] extraordinary transmission through subwavelength apertures in thin metal film,[6,7] and subwavelength waveguiding in metal nanostructures.[8−10] Plasmonics is gaining immense interest because of the potential applications of the above-mentioned phenomena in nano-optical components for plasmonic circuits,[11,12] fabrication of nanoscale structures,[13,14] photovoltaics,[15,16] and chemical/biological sensors.[17]

The time varying electric field of the electromagnetic radiation causes oscillation of conductive electrons in metal nanoparticles. The resonance of such oscillation, termed localized surface plasmon resonance (LSPR), falls into the visible regime for noble metals such as gold and silver. LSPR of metal nanostructures is sensitive to numerous factors such as composition, size, shape, dielectric ambient, and proximity to other nanostructures (plasmon coupling).[18,19] The sensitivity of LSPR to localized changes in dielectric environment renders it an attractive transduction platform for chemical and biological sensing.[20−24] LSPR overcomes the deficiencies of the conventional SPR approach because eof the simplicity of exciting surface plasmons in metal nanostructures and the ability to address the same down to single nanostructures enabling high lateral resolution and single molecule detection.[25,26]

Responsive plasmonics, which involves dynamic tuning of the plasmonic properties of metal nanostructures and their assemblies, is an exciting fundamental challenge with potential applications in sensing, optoelectronics and adaptive materials. One reliable way to approach this challenge is to use responsive polymers, which exhibit large changes in conformation with external stimuli such as pH, temperature, electric field, and magnetic field.[27−33] It is known that the plasmonic coupling between metal nanoparticles is extremely sensitive to the distance of separation between the nanoparticles, which is exploited in plasmon ruler.[34] Recent experimental and theoretical investigation suggests that the plasmon coupling strength decays exponentially with separation distance.[35] The large change in the dimensions of the responsive polymer chains with external stimuli is translated to change in distance of separation between the nanostructures, which in turn tunes the strength of the plasmonic coupling. Numerous polymer/nanoparticle hybrid structures such as cross-linked thin films, layer-by-layer assembled films, polymer brushes, core−shell structures, block copolymer nanotubes have been investigated.[36−39] However, in most of these cases the tunability of the plasmonic properties remains rather limited due

Received: January 26, 2011
Accepted: March 7, 2011
Published: March 07, 2011

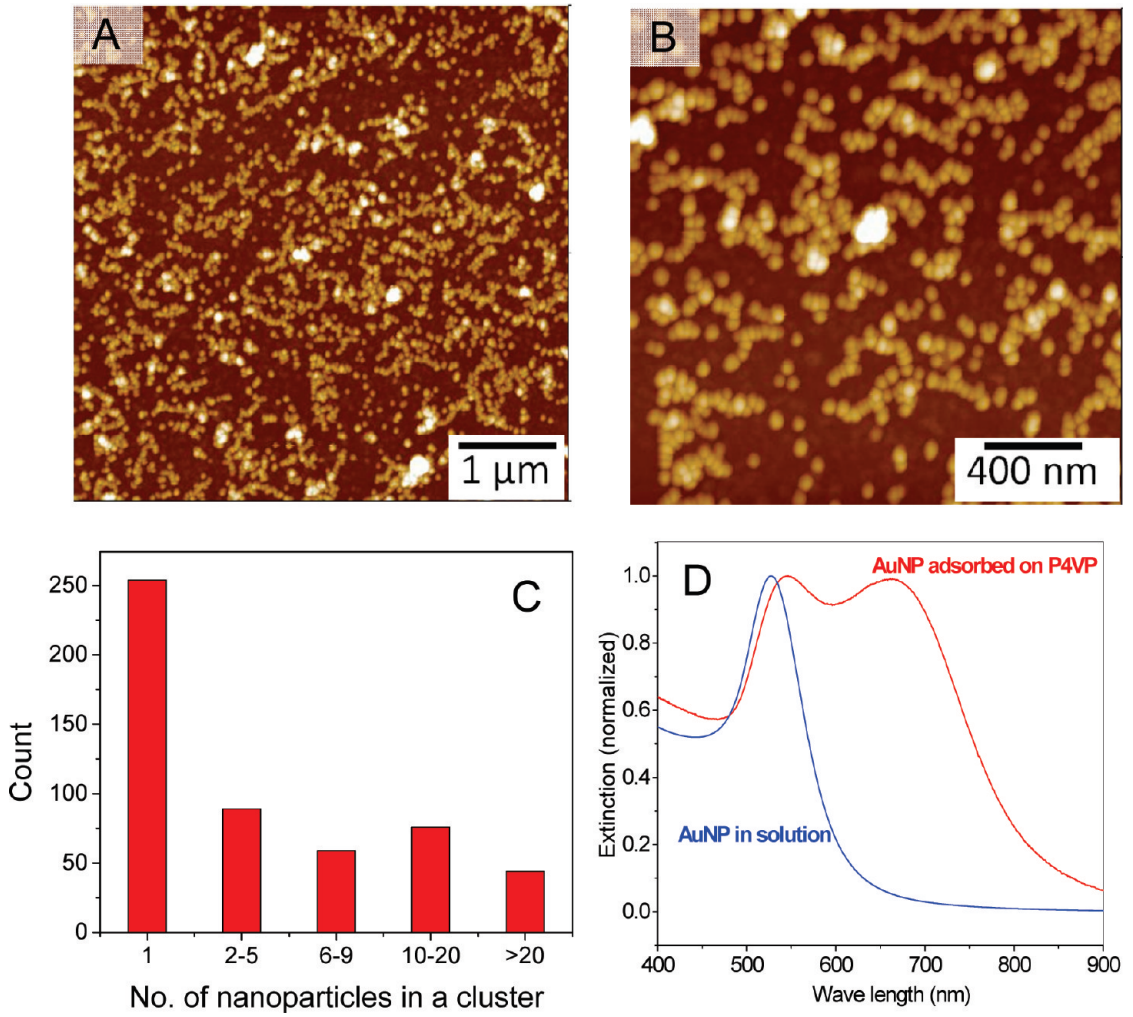

Figure 1. AFM images showing the (A) large-scale surface morphology of the gold nanoparticles adsorbed on the P4VP film (B) higher-resolution image showing the linear and branched nanoparticle chains (C) Histogram showing the distribution of the nanoclusters comprised of different number of nanoparticles (D) UV−visible extinction spectra of the nanoparticle solution and the nanoparticle chain aggregates formed on the surface of the P4VP film.

to the isotropic nature of the nanoparticle aggregates formed in the collapsed (globule) state of the polymer chains.

In this work, we demonstrate the deployment of an ultrathin (∼1 nm thick) and un-cross-linked responsive polymer layer to achieve large and reversible plasmonic tuning of metal nanostructure assemblies. More importantly, the plasmonic tunability of nanoparticle chains was found to be higher compared to that of individual nanoparticles and isotropic aggregates. The large changes in the conformation of adsorbed poly (4-vinyl pyridine) (P4VP) layer result in reversible formation of linear and branched chains of nanoparticles and concomitant change in the optical properties associated with the plasmon coupling.

P4VP is a weak cationic polymer which exhibits a coil to globule transition at around pH 3.5.[40] Ultrathin polymer layer was adsorbed onto a substrate from P4VP solution (in ethanol) followed by extensive rinsing with copious amount of ethanol (see Experimental Section for details). The polymer layer exhibited uniform and featureless surface morphology with root-mean-square (rms) roughness of ∼0.5 nm over 1 × 1 μm^2 (see the Supporting Information, Figure S1). The thickness of the adsorbed P4VP layer was found to be ∼1 nm using AFM scratch test (see the Supporting Information, Figure S2). Gold nanoparticles with diameter of 25.8 ± 3.8 nm were synthesized using citrate mediated reduction of gold salt (see Experimental Section). The nanoparticles under normal pH conditions had a modest negative charge on the surface.

Figure 1A, B show AFM images of the nanoparticles adsorbed on the P4VP film. Majority of the nanoparticles (∼92%) were found to exist as single nanoparticle wide linear or branched chains rather than as individual nanoparticles. Earlier studies involving the adsorption of citrate-stabilized gold nanoparticles onto polyelectrolyte multilayers indicated similar chains of nanoparticles.[41,42] The chains comprised 10−40 nanoparticles and were formed during the solvent evaporation. The AFM images revealed very few isotropic (close packed nanoparticles) aggregates and almost no large vertical aggregates. Figure 1C shows the histogram of the distribution of nanoclusters with different number of nanoparticles.

Figure 1D shows the extinction spectrum of gold nanoparticles in solution and adsorbed on the surface of the P4VP film. Extinction spectrum of gold nanoparticles in solution shows the characteristic plasmon absorption band of the gold nanoparticles with peak at 527 nm. On the other hand, the extinction spectra of

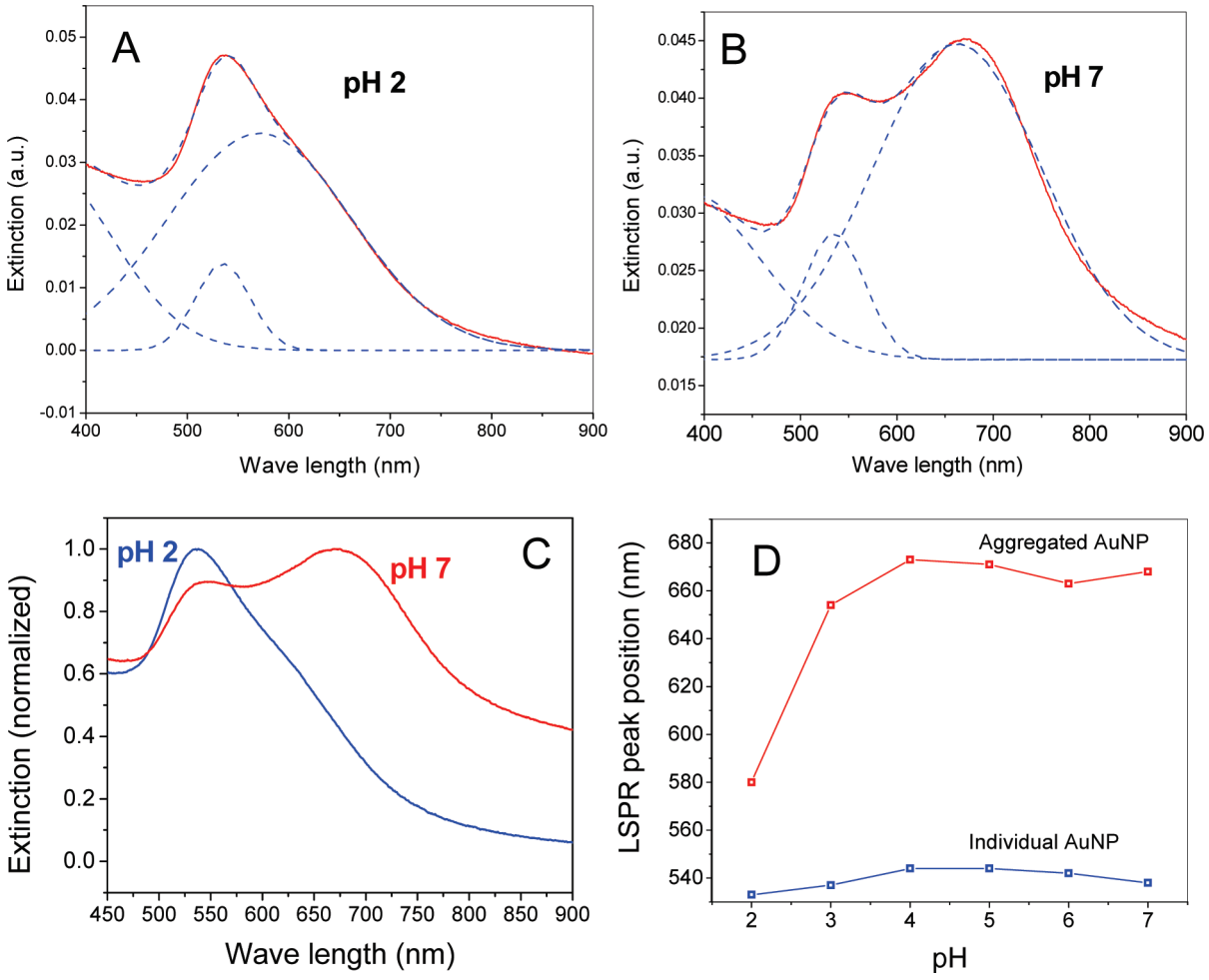

Figure 2. Representative extinction spectra of the AuNP on P4VP film at (A) pH2 and (B) pH 7 with peak deconvolution using three Gaussian peaks. (C) Normalized extinction spectra at pH 2 and pH 7 showing the redistribution of the peak intensity between the individual and coupled plasmon bands and the large red shift in the coupled plasmon band. (D) Plot showing the peak position of the individual and coupled plasmon bands at different pH.

the nanoparticles adsorbed on the P4VP shows two distinct bands centered at 537 and 660 nm. The peak at 537 nm corresponds to the individual nanoparticles and the transverse surface plasmon mode of linear AuNP chains while the band centered at 660 nm corresponds to the longitudinal surface plasmon mode of the nanoparticle chains with strong plasmon coupling.[43] The extinction spectrum is in agreement with the AFM images, which revealed high fraction of AuNP as linear chains. It has been demonstrated that linear aggregation of the nanoparticles results in the appearance of the higher wavelength band, the position of which depends on the length of the linear chains.[44] It is also known that the higher wavelength band (called coupled plasmon band henceforth) exhibits a progressive red shift as the length of the nanoparticle chain increases. The coupled plasmon band peak was found to be broader compared to that of the individual nanoparticles at 537 nm. The relatively broad peak indicates the polydispersity in the length of the nanoparticle chains formed on the P4VP film, which is in agreement with the AFM observation discussed above (Figure 1C). The individual nanoparticle plasmon band of the AuNP adsorbed on the substrate was found to be slightly red-shifted (10 nm) compared to that in solution, which can be ascribed to the change in the refractive index (water vs air+substrate).[45]

Spectra A and B in Figure 2 show the extinction spectra of the gold nanoparticles on the P4VP layer at pH 2 and pH 7, respectively. The individual and coupled plasmon bands have been deconvoluted by fitting the extinction spectrum with three Gaussian peaks as shown in the plot. A dramatic redistribution of the intensity between the individual nanoparticles and aggregated nanoparticles bands can be observed at the two different pH conditions (Figure 2C). At pH 2, the individual nanoparticle plasmon band (at 537 nm) was found to be significantly stronger than the higher wavelength band, which appeared as a shoulder at 580 nm. On the other hand, at pH 7, the intensity of higher wavelength band was found to be slightly stronger than the individual nanoparticle plasmon band. Apart from the large redistribution in the intensity of between the two bands, both the plasmon bands exhibited a red shift in the peak position at pH 7 compared to that at pH 2. The individual nanoparticle band was found to red shift by ~10 nm while the coupled plasmon band exhibited much larger shift (~93 nm). The shift in the coupled plasmon resonance observed here is significantly higher than the previous demonstrations involving responsive polymer systems for tunable plasmonics.[36,38,39] We believe that the unique nanoparticle morphology i.e. chains of nanoparticles as opposed to the randomly distributed or closely packed nanoparticles in

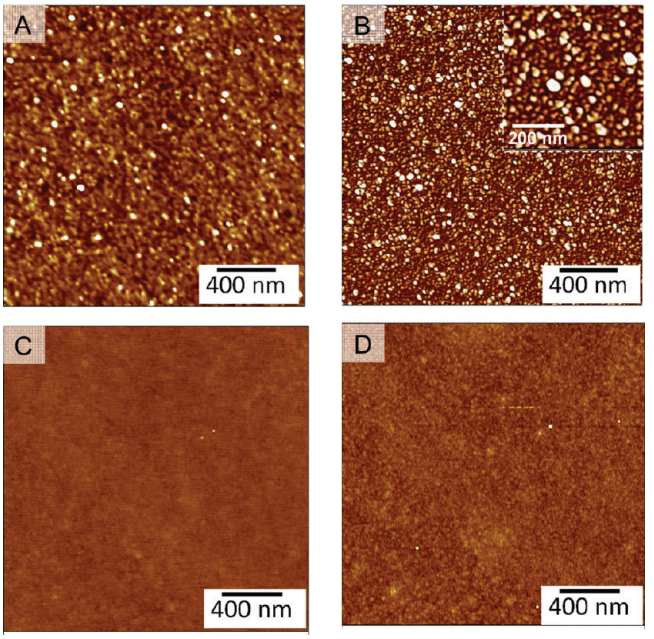

Figure 3. Topography and phase images of adsorbed P4VP film exposed to (A, B) pH 7 and (C, D) pH 2 showing the grainy globular morphology and the coiled featureless surface morphology, respectively. Z-scale of the images A and C: 10 nm, B: 40° and D: 5°.

most of the previous demonstrations resulted in the enhanced plasmon resonance. Furthermore, the un-cross-linked state of the adsorbed polymer layer facilitates larger changes in the dimensions of the polymer chains resulting in larger tunability of the plasmonic properties of the nanoparticle assemblies.

Figure 2D shows the plasmon tuning with change in the external pH. The peak position of both individual and coupled plasmon bands exhibited a red shift with increase in the external pH. The shift in the coupled plasmon band position with change in external pH exhibited a smooth curve with most dramatic changes occurring at around pH 3.0, which closely corresponds to the isoelectric point of P4VP (pH 3.2).[40] The larger shift in the longitudinal band can be ascribed to the higher shape factor of the chains of nanoparticles compared to the individual particles. It has been recently demonstrated that the pairs of nanoparticles with higher shape factor exhibit higher refractive index sensitivity compared to the individual nanoparticles.[46] Redistribution of the intensity between the individual and coupled plasmon bands showed similar trend with most dramatic changes happening between pH 2.5 and 3.5, which corresponds to the protonation of the P4VP chains and transition from coil to globule state. It is known that change in external pH results in the large change in the molecular dimensions of the P4VP chains (coil to globule transition). The nanoparticles adsorbed on the responsive polymer chains also follow the structural changes of the polymer chains.

AFM imaging was employed to understand the structural changes in adsorbed polymer layer exposed to different pH conditions. Figure 3 shows the AFM topography and phase images of the P4VP film following the exposure to pH 2 (and pH 7) and subsequent rapid drying of the samples. While the surface morphology of the film exposed to pH 7 exhibited nanoscale grainy surface morphology, the film exposed to pH 2 exhibited uniform, smooth and featureless morphology (see Figure 3A,C). The grainy and smooth morphology of the P4VP surface exposed to pH 7 and 2, respectively, is clearly evident from the phase images B and D in Figure 3. The radius of the individual grains observed in the phase image was found to be 15−25 nm (after accounting for the AFM tip dilation). The radius of the polymer grains observed here closely agrees with the radius of gyration of individual poly(2-vinyl pyridine) globules of similar molecular weight reported earlier.[47] The rms surface roughness (over $1 \times 1\ \mu m^2$ area) of the surface exposed to pH 7 (0.6 nm) was significantly higher than the P4VP surface exposed to pH 2 (0.25 nm). The morphology was found to be completely reversible between the grainy and smooth featureless states with exposure to different pH conditions.

AFM imaging was also performed on P4VP film with Au NP following the exposure to pH 7 (Figure 4A,B) and pH 2 (Figure 4C,D). AFM images revealed that exposure to pH 2 causes the nanoparticles to be primarily in individual state as opposed to primarily linear and branched chains in the pristine sample. The swelling of the P4VP chains upon exposure to acidic conditions results in the breaking of the linear aggregates and resulting in isolated nanoparticles. A careful observation of the AFM image reveals that the nanoparticles still exist as linear chains (highlighted in the AFM image) after exposure to pH 2 but with larger spacing between them (highlighted in Figure 4D). It is important to note that the AFM images were obtained in the dry state following the exposure to pH 2 and subsequent rapid drying of the polymer. The swelling effects observed in the polymer are only residual effects during rapid drying of the polymer. On the other hand, P4VP-Au NP sample exposed to pH 7 showed significantly higher number of particles in proximity to other nanoparticles and in chain aggregates.

Figure 4E shows the plot of the number of particles observed in chains comprised of different number of particles. The plot clearly reveals that the fraction of individual nanoparticles observed in sample exposed to pH 2 (44% of the total number of particles) is more than twice of the same observed in samples exposed to pH 7 (19% of the total number of particles). On the other hand, the fraction of nanoparticles in clusters is significantly higher in the sample exposed to pH 7 compared to the sample exposed to pH 2. The clusters were primarily chain aggregates of nanoparticles in both cases.

AFM images clearly reveal the pH induced reversible changes in the morphology of the P4VP film and the associated changes in the aggregation state of the nanoparticles. Figure 4F shows the proposed mechanism responsible for the observed large changes in the optical properties of the Au NP adsorbed on the P4VP film. In protonated state (below isoelectric point), the P4VP chains exist as extended coils, resulting in weakly interacting nanoparticles. On the other hand, at higher pH (above isoelectric point) the polymer chains primarily exist as collapsed globules and the nonaoparticles on the top are drawn closer forming strongly interacting linear and branched chains.[40] Apart from the changes in the plasmon coupling, the local refractive index changes also contribute to the observed change in the optical properties. Dramatic changes in refractive index of temperature responsive gels at phase transition (lower critical solution temperature) have been observed using surface plasmon resonance and optical waveguide spectroscopy.[48] The transition of the polymer chains from swollen coiled state (with water) to collapsed globule state (absence of water) results in an increase of the effective refractive index experienced by the nanoparticles. It is known that the plasmon resonance of the nanoparticles exhibits a red shift with

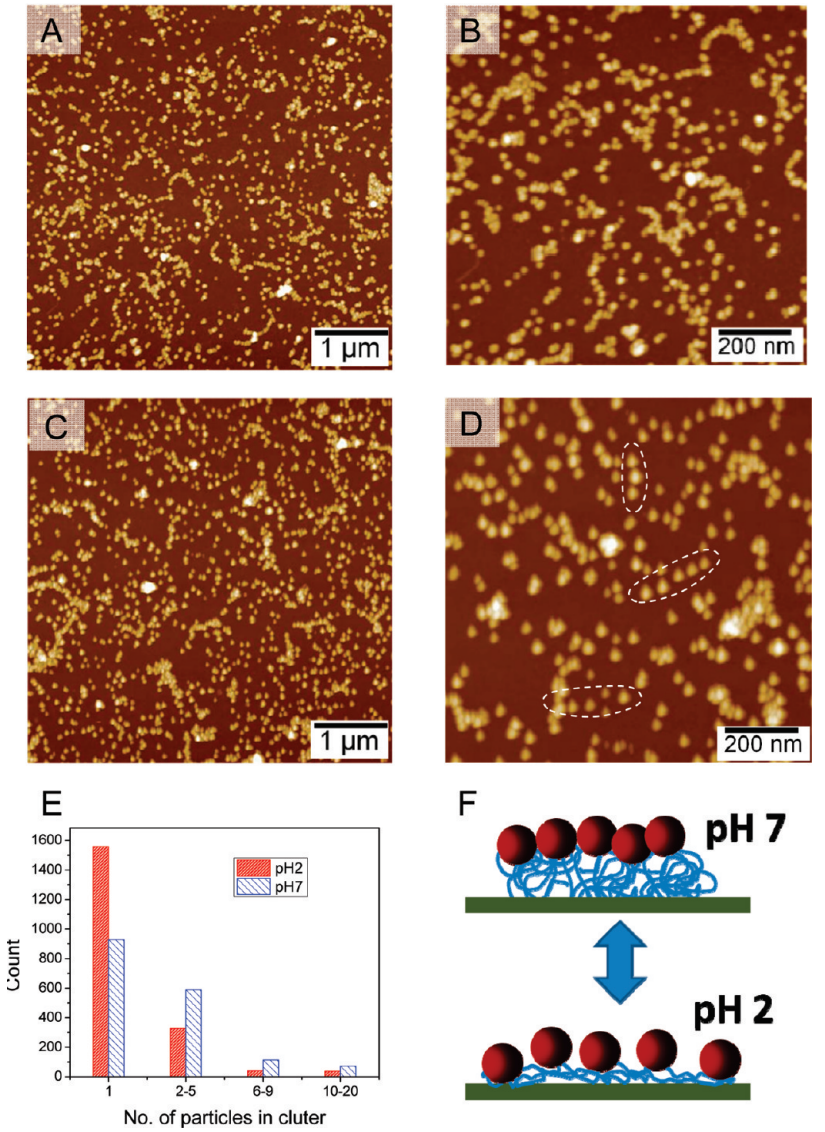

Figure 4. AFM images of Au NP adsorbed P4VP after exposure to (A, B) pH 7 and (C, D) pH 2 (E) Histogram showing the number of particles in nanoclusters after exposure to pH 2 and pH 7. (F) Schematic showing coil to globule transition of the adsorbed polymer chains and the associated change in spacing between the nanoparticles in the chain aggregates.

increase in the refractive index, which augments the plasmon coupling effect.[49]

To probe the reversibility of the observed tunable plasmonic effects, we exposed the nanoparticle chains on the responsive polymer to cycles of pH 2 and 7. The peak position of the coupled plasmon band follows the changes in the pH (Figure 5A). The peak position exhibited a large shift (~90 nm) when the pristine sample was exposed to pH2 and subsequent cycles showed smaller shift (~40 nm). AFM images discussed above also support this observation (see Figures 1A–C and 4A–E). The linear chains in the pristine sample are comprised of nearly 20–30 nanoparticles. Upon exposure to pH2, the nanoparticles chains break to mostly non-interacting isolated nanoparticles. Subsequent exposure to pH7 resulted in the formation of chains comprised of 5–10 nanoparticles, which are significantly shorter compared to the pristine sample. A small blue drift (5–10 nm) in the peak position was observed in the first two cycles due the decrease in the length of the chains. Figure 5B shows the intensity ratio of individual plasmon band and coupled plasmon band. The intensity ratio of both the bands also shows clear variation between the two distinct values with small variation (<20%) over four consecutive cycles. The cycling results clearly demonstrate the reversibility and stability of the plasmon tuning that can be achieved by the ultrathin adsorbed responsive polymer layer.

In conclusion, we have demonstrated tunable, reversible and a highly sensitive surface plasmonic response of linear chainlike Au NP aggregates adsorbed on an ultrathin responsive polymer film. The simple and efficient method suggested here enables large tunability in optical properties, obviating the need for complex nanofabrication such as layer-by-layer assembly, template assisted assembly, polymer brushes or any chemical modification of nanostructures. We believe that the un-cross-linked nature of the polymer chains is critical for large changes in polymer chain conformation and hence large tunability of the plasmonic properties. The observed plasmonic tunability of AuNP chains can be extended to other shape-controlled nanostructures such as nanorods, nanocubes, and bipyramids. The approach suggested

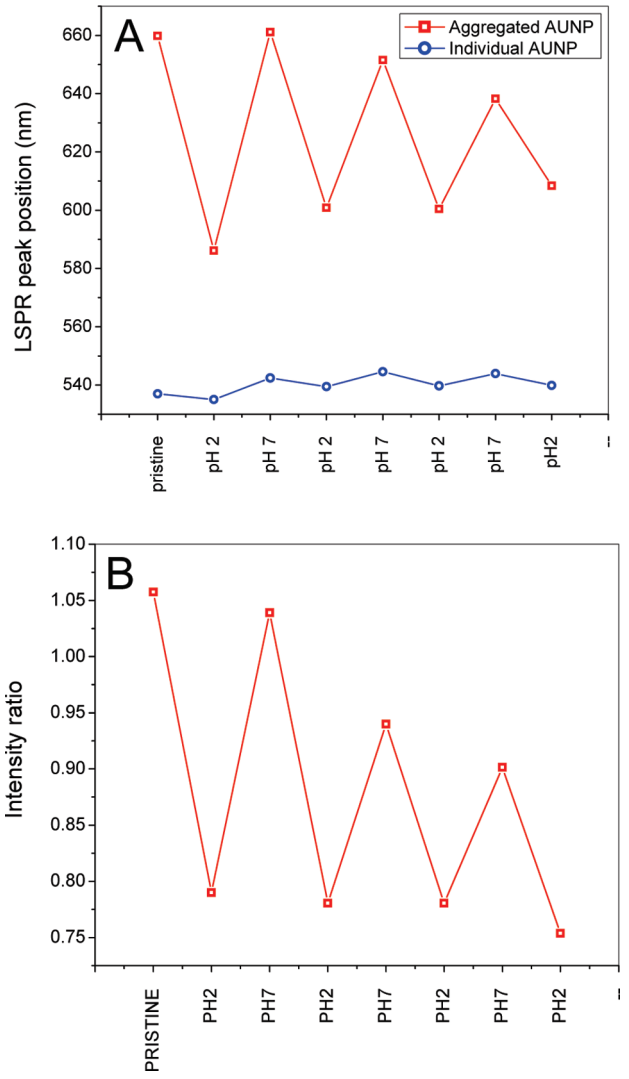

Figure 5. (A) Plot showing the peak position of the individual and coupled plasmon bands band aggregated with external pH cycled between 2 and 7. (B) Plot showing the intensity ratio of the coupled plasmon band and the individual plasmon band with external pH cycled between 2 and 7.

here can find important applications in developing highly sensitive chemical and biological sensors, optoelectronic devices and adaptive materials.

EXPERIMENTAL SECTION

Gold nanoparticles were synthesized according the procedure described in the literature.[50] In brief, 1.0 mL of a 1% sodium citrate solution (in nanopure water (18.2 MΩ cm)) was quickly injected into 100 mL of boiling 0.01% aqueous $HAuCl_4$ solution. The solution was kept under boiling conditions for 10 min and continuously stirred for an additional 15 min. Gold nanoparticle solutions were stored at room temperature in a dark area and used within 3 weeks. These nanoparticles bear a modest negative charge under normal pH conditions and remain stable in solution for several weeks.

Glass substrates were cut into approximately 1 × 2 cm^2 rectangular slides and cleaned in piranha solution (3:1 (v/v) mixture of H_2SO_4 and 30% H_2O_2) followed by extensive rinsing with Nanopure water (18.2 MΩ cm). Adsorption of P4VP was achieved by immersing a glass substrate in 4% P4VP solution in ethanol for 60 min followed by washing with copious amounts of ethanol. Au NP solution (20 μL) was drop-casted on P4VP film and evaporated naturally under room conditions. Sample was washed with Nanopure water to remove weakly adsorbed nanoparticles and any large vertical aggregates that formed during the course of evaporation. It is worth noting that the amount of AuNP drop casted is critical for achieving the large optical response observed here. Smaller amounts resulted in very few chains and mostly individual particles, which is not ideal for responsive plasmonics. On the other hand, larger amounts resulted in isotropic and large number of vertical aggregates, which exhibited poor response to pH. An alternate approach involving spin-casting composite polymer solution (100 μL AuNP solution in 0.5 mL of 4% P4VP in ethanol) resulted in microscale phase separation with no sign of nanoparticle chains (see the Supporting Information, Figure S3).

UV−vis extinction spectra were collected using Shimadzu 1800 spectrophotometer. The extinction spectra of the AuNP chains were measured in wet state by immersing the substrate in solution at different pH. Solutions with different pH were prepared by adjusting the pH (dropwise addition) of nanopure water using dilute HCl (0.1 M) or 0.1% NaOH and used immediately after preparation. AFM images were collected in tapping mode using standard silicon nitride cantilevers using Dimension 3000 AFM (Veeco). The thickness of the polymer film was measured by using scratch test, which involved making scratch on the polymer film using a sharp scribe followed by scanning along the edge of the scratch (see the Supporting Information, Figure S2).

ASSOCIATED CONTENT

Supporting Information. AFM images showing the surface morphology of the P4VP layer adsorbed on silicon surface, AFM scratch test showing the thickness of the adsorbed P4VP layer to be approximately 1 nm and the representative AFM images of the spin-cast composite solution. This material is available free of charge via the Internet at http://pubs.acs.org.

AUTHOR INFORMATION

Corresponding Author
*E-mail: singamaneni@wustl.edu.

ACKNOWLEDGMENT

We thank Dr. Chang H. Lee and Dr. Ramesh Kattumenu for technical assistance. The work reposted was supported by the start up funds from Washington University and a seed grant from Siteman Cancer Center and Center for Materials Innovation.

REFERENCES

(1) Maier, M. S. *Plasmonics: Fundamentals and Applications*, 1st ed.; Springer: New York, 2007.
(2) Ozbay, E. *Science* **2006**, *311*, 189–193.
(3) Hao, E.; Schatz, G. C. *J. Chem. Phys.* **2004**, *120*, 357–366.
(4) Gersten, J.; Nitzan, A. *J. Chem. Phys.* **1980**, *73*, 3023–3037.
(5) Willets, K. A.; Van Duyne, R. P. *Annu. Rev. Phys. Chem.* **2007**, *58*, 267–297.
(6) Barnes, W. L.; Dereux, A.; Ebbesen, T. W. *Nature* **2003**, *424*, 824–830.
(7) Ebbesen, T. W.; Lezec, H. J.; Ghaemi, H. F.; Thio, T.; Wolff, P. A. *Nature* **1998**, *391*, 667–669.
(8) Ditlbacher, H.; Hohenau, A.; Wagner, D.; Kreibig, U.; Rogers, M.; Hofer, F.; Aussenegg, F. R.; Krenn, J. R. *Phys. Rev. Lett.* **2005**, *95*, 257403(4).

(9) Pyayt, A. L.; Wiley, B.; Xia, Y.; Chen, A.; Dalton, L. *Nature Nanotechnol.* **2008**, *3*, 660–665.
(10) Lal, S.; Link, S.; Halas, N. J. *Nat. Photonics* **2007**, *1*, 641–648.
(11) Nikolajsen, T.; Leosson, K.; Bozhevolnyi, S. I. *Appl. Phys. Lett.* **2004**, *85*, 5833–5835.
(12) Cai, W.; White, J. S.; Brongersma, M. L. *Nano Lett.* **2009**, *9*, 4403–4411.
(13) Srituravanich, W.; Pan, L.; Wang, Y.; Sun, C.; Bogy, D. B.; Zhang, X. *Nature Nanotechnol.* **2008**, *3*, 733–737.
(14) Rontzsch, L.; Heinig, K. H.; Schuller, J. A.; Brongersma, M. L. *Appl. Phys. Lett.* **2007**, *90*, 044105(3).
(15) Stenzel, O.; Stendal, A.; Voigtsberger, K.; von Borczyskowski, C. *Sol. Energy Mater. Sol. Cells* **1995**, *37*, 337–348.
(16) Atwater, H. A.; Polman, A. *Nat. Mater.* **2010**, *9*, 205–213.
(17) Anker, J. N.; Hall, W. P.; Lyandres, O.; Shah, N. C.; Zhao, J.; Van Duyne, R. P. *Nat. Mater.* **2008**, *7*, 442–453.
(18) Rosi, N. L.; Mirkin, C. A. *Chem. Rev.* **2005**, *105*, 1547–1562.
(19) Reinhard, B. M.; Siu, M.; Agarwal, H.; Alivisatos, A. P.; Liphardt, J. *Nano Lett.* **2005**, *5*, 2246–2252.
(20) Sepulveda, B.; Angelome, P. C.; Lechuga, L. M.; Liz-Marzán, L. M. *Nano Today* **2009**, *4*, 244–251.
(21) Haes, A. J.; Van Duyne, R. P. *J. Am. Chem. Soc.* **2002**, *124*, 10596–10604.
(22) Riboh, J. C.; Haes, A. J.; McFarland, A. D.; Yonzon, C. R.; Van Duyne, R. P. *J. Phys. Chem. B* **2003**, *107*, 1772–1780.
(23) Yonzon, C. R.; Jeoung, E.; Zou, S.; Schatz, G. C.; Mrksich, M.; Van Duyne, R. P. *J. Am. Chem. Soc.* **2004**, *126*, 12669–12676.
(24) Haes, A. J.; Chang, L.; Klein, W. L.; Van Duyne, R. P. *J. Am. Chem. Soc.* **2005**, *127*, 2264–2271.
(25) Nie, S. M.; Emory, S. R. *Science* **1997**, *275*, 1102–1106.
(26) Mayer, K. M.; Hao, F.; Lee, S.; Nordlander, P.; Hafner, J. H. *Nanotechnology* **2010**, *21*, 255503.
(27) Stuart, M. A. C.; Huck, W. T. S.; Genzer, J.; Muller, M.; Ober, C.; Stamm, M.; Sukhorukov, G. B.; Szleifer, I.; Tsukruk, V. V.; Urban, M.; Winnik, F.; Zauscher, S.; Luzinov, I.; Minko, S. *Nat. Mater.* **2010**, *9*, 101–113.
(28) Liu, F.; Urban, M. W. *Prog. Polym. Sci.* **2010**, *35*, 3–23.
(29) Kumar, A.; Srivastava, A.; Galaev, I. Y.; Mattiasson, B. *Prog. Polym. Sci.* **2007**, *32*, 1205–1237.
(30) Richter, A.; Paschew, G.; Klatt, S.; Lienig, Arndt, K. F.; Adler, H. J. P. *Sensors* **2008**, *8*, 561–581.
(31) Hu, J.; Liu, S. Y. *Macromolecules* **2010**, *43*, 8315–8330.
(32) Meng, H.; Hu, J. L. *J. Intell. Mater. Syst. Struct.* **2010**, *21*, 859–885.
(33) Mano, J. F. *Adv. Eng. Mater.* **2008**, *10*, 515–527.
(34) Sonnichsen, C.; Reinhard, B. M.; Liphardt, J.; Alivisatos, A. P. A *Nat. Biotechnol.* **2005**, *23*, 741–745.
(35) Jain, P. K.; Huang, W.; El-Sayed, M. A. *Nano lett.* **2007**, *7*, 2080–2088.
(36) Tokarev, I.; Tokareva, I.; Minko, S. *Adv. Mater.* **2008**, *20*, 2730–2734.
(37) Tokareva, I.; Minko, S.; Fendler, J. H.; Hutter, E. *J. Am. Chem. Soc.* **2004**, *126*, 15950–15951.
(38) Kozlovskaya, V.; Kharlampieva, E.; Khanal, B. P.; Manna, P.; Zubarev, E. R.; Tsukruk, V. V. *Chem. Mater.* **2008**, *20*, 7474.
(39) Chang, S.; Singamaneni, S.; Kharlampieva, E.; Young, S. L.; Tsukruk, V. V. *Macromolecules* **2009**, *42*, 5781–5785.
(40) Li, D.; He, Q.; Cui, Y.; Li, J. *Chem. Mater.* **2007**, *19*, 412–417.
(41) Jiang, C.; Markutsya, S.; Tsukruk, V. V. *Langmuir* **2004**, *20*, 882–890.
(42) Jiang, C.; Lio, W. Y.; Tsukruk, V. V. *Phys. Rev. Lett.* **2005**, *95*, 115503(4).
(43) Maier, S. A.; Kik, P. G.; Atwater, H. A. *Appl. Phys. Lett.* **2002**, *81*, 1714–1716.
(44) Lin, S.; Li, M.; Dujardin, C. G.; Mann, S. *Adv. Mater.* **2005**, *17*, 2553–2559.
(45) Malinsky, M. D.; Kelly, K. L.; Schatz, G. C.; Van Duyne, R. P. *J. Phys. Chem. B* **2001**, *105*, 2343–2350.
(46) Jain, P. K.; El-Sayed, M. *Nano lett.* **2008**, *8*, 4347–4352.
(47) Roiter, Y.; Minko, S. *J. Am. Chem. Soc.* **2005**, *127*, 15688–15689.
(48) Harmon, M. E.; Kuckling, D.; Frank, C. W. *Macromolecules* **2003**, *36*, 162–172.
(49) Nath, N.; Chilkoti, A. *Anal. Chem.* **2004**, *76*, 5370–5378.
(50) Grabar, K. C.; Freeman, R. G.; Hommer, M. B.; Natan, M. J. *Anal. Chem.* **1995**, *67*, 735–743.